IEEE Transactions on Nuclear Science, Vol. NS-26, No. 3, June 1979

TEST ACCUMULATION RING FOR NUMATRON PROJECT — TARN —

Y. Hirao, K. Chida, T. Hattori, T. Hori, T. Katayama, A. Mizobuchi, M. Mutou, T. Nakanishi, A. Noda, K. Omata, N. Tokuda, H. Tsujikawa, S. Watanabe, S. Yamada, M. Yoshizawa, E. Ezura,*) H. Sasaki*) and A. Miyahara**)

Institute for Nuclear Study, University of Tokyo, Tokyo, Japan

Abstract

A Test Accumulation Ring for NUMATRON Project, TARN, is now under construction at INS, University of Tokyo. Heavy ions from the SF Cyclotron such as N^{5+} with an energy of 8.5 MeV per nucleon, are planned to be injected and stacked in the ring by a combination of multiturn injection and RF stacking method. Expected intensity of the stacked beam, e.g. N^{5+}, is 2×10^{10} particles, and a survival rate of 90 % is anticipated at the pressure of 1×10^{-10} torr during a stacking time of 1 sec. In this paper, the present status of the ring is described as well as the performances of the major subsystems.

1. Introduction

Recently, interests in high-energy heavy-ions have grown up not only in the field of nuclear physics but also in the scientific communities of solid state Physics, medical biology, and fusion power generation engineering. In Japan, an accelerator for high-energy heavy-ion, NUMATRON,[1,2] was projected at INS, University of Tokyo. At the design of the accelerator, a synchrotron with an accumulation ring is most preferable for obtaining an expected high intensity beam of heavy ions, considering a present ion source technology and a low duty factor of synchrotron.

The Test Accumulation Ring for NUMATRON, TARN, is being constructed at INS for developing technical subjects related to the heavy ion accelerator complex. The heavy ion beams, for example N^{5+} of 8.5 MeV/u, from the INS-SF Cyclotron[3] are injected and accumulated in the TARN, as shown in Fig.1. The injector cyclotron is a multi-particle variable-energy accelerator and has been in operation since 1974. A cold cathode PIG source for heavy ions was developed and extracted beams of 4.3 μA $^{14}N^{5+}$ and 1.5 μA $^{20}Ne^{6+}$ are obtained.[4]

The main parameters of the TARN are given in Table 1. The ring consists of eight bending magnets and sixteen quadrupole magnets with a lattice structure of FODO type. The mean radius is 5.06 m and the bending radius of the central oribt is 1.333 m. The overall ring view is shown in Fig.2. The heavy ion beam is accelerated in the SF Cyclotron and introduced in the ring via a beam transporting path, and is injected in the ring by a combination of multiturn injection and RF stacking method. Expected intensity of accumulated ions such as N^{5+} is more than 2×10^{10} particles. The life time of the stacked beam is determined mainly by the charge exchange reactions between heavy ions and residual gas molecule. Assuming the cross section of the reactions of 2.80×10^{-17} cm^2, the required pressure in the ring is 1×10^{-10} torr for the survival rate of 90 % during a stacking time of 1 sec. At present major parts of the ring are completed and the first beam injection will be done in coming May. In following sections, design and performances of the ring and major subsystems are described.

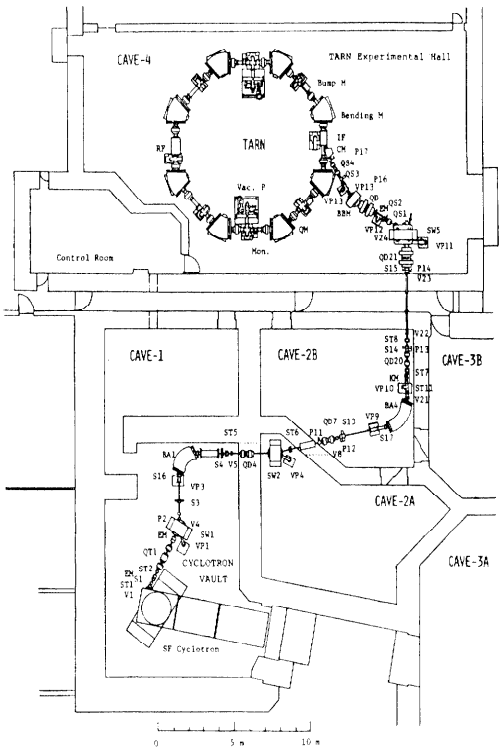

Fig.1. Layout of the TARN and the beam transport system from the SF Cyclotron. BA : Analyzer magnet. BBM : Bending magnet. SW : Switching magnet. Q : Quadrupole magnet. ST : Steering magnet. KM : Kicker magnet. S : Slit system. EM : Emittance monitor. P : Profile monitor. VP : Pumping system.

2. Magnetic Focusing System

Lattice Structure and Aperture Requirement

Focusing structure of the TARN is an FODO type of a separated function, where both the superperiodicity and the number of normal cells are eight. The mean radius and the circumference of the ring are 5.06 m and 31.795 m, respectively, which were determined considering the synchronization between two RF systems of the TARN with a harmonic number of seven and of the injector cyclotron. The number of betatron oscillation per revolution is 2.25 both in horizontal and vertical directions.

The required useful apertures in the horizontal direction are determined as 85 mm in half side both in the bending magnet and quadrupole magnet, considering the amplitude of betatron oscillation, closed orbit displacement and the spread of closed orbit due to momentum spread of the stacked beam. The calculations were based upon the assumption that the beam emittance in horizontal direction after multiturn injection was 40 π mm·mrad and the momentum spread of the stacked beam was 2.47 %. The beam emittance in vertical direction was assumed to be 20 π mm·mrad including the effect of injection errors. In the bending magnet, the

*) National Laboratory for High Energy Physics (KEK), Ibaragi, Japan.
**) Institute of Plasma Physics, Nagoya University, Nagoya, Japan.

0018-9499/79/0600-3730$00.75 © 1979 IEEE

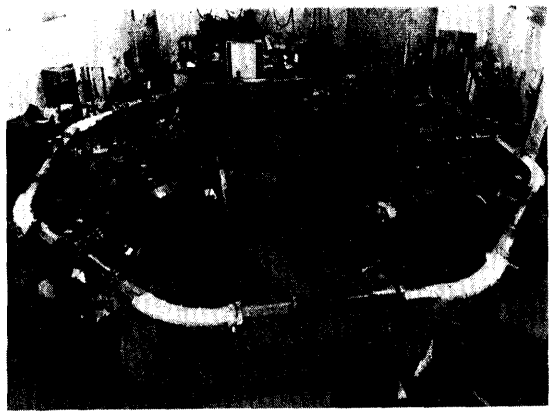

(a)

(b)

Fig.2. View of the TARN under construction. (a) Vacuum system, arranged tentatively before the installation into the magnet gaps. (b) Bending and quadrupole magnets.

vertical amplitude of betatron oscillation, closed orbit displacement and clearance are 8.34 mm, 3.1 mm and 8.56 mm in half side respectively, and the required vertical useful aperture is 20 mm in half side. In the quadrupole magnet, the corresponding values are 10.47, 4.0 and 5.53 mm in half side, and the required useful aperture in vertical directions is also 20 mm in half side. The apertures of the magnets were determined with the consideration of the thickness of the vacuum chamber wall, 4 mm, and spaces for heat insulation elements and distributed ion pumps. The aperture of the bending magnet was 70 (height) × 258 (width) mm^2 and the bore radius of the quadrupole magnet was 65 mm.

Magnet Construction and Field Measurements

The bending magnet is a window-frame type, which has merits of compactness of the structure and good field uniformity. In order to avoid the sagitta due to the small radius of curvature, 1.333 m, the magnet is fan-shaped. The edges of the magnet pole at both ends were designed to be normal to the central orbit. In order to reduce the flux density at the edge of iron yoke, the pole edges were cut with four steps approximating the Rogowski's curve. The shielding plates were attached at both ends considering the small distance between the bending magnet and quadrupole magnets.

The qudrupole magnet was designed to afford the possibility of AC operation in the case of fast tuning of ν-values. The shape of the pole was determined using the computer program TRIM and it was consisted of a hyperbola which extended to its tangential line at both sides. The mechanical pole edge was cut so as to enlarge the flat region of the effective focusing strength.

The magnetic fields of the eight bending magnets were measured with a temperature-controlled Hall probe with a precision of better than 1 G. The probe was automatically positioned by a computer-controlled driving system. The excitation characteristics of each magnet was measured with an NMR probe inserted into the magnet gap

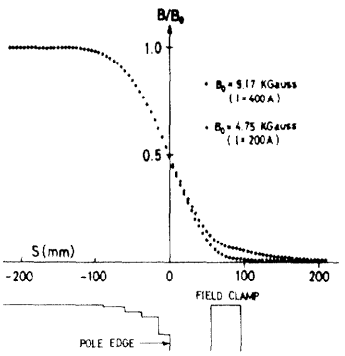

Fig.3. The distribution of the magnetic field along the beam orbit near the pole edge of the bending magnet. The effective edge was calculated according to these curves.

Table Parameter List of the TARN

General	
Beam energy (for N^{5+})	8.56 MeV/u
Magnetic field	B = 8.574 kG
Bending radius	ρ = 1.333 m
Mean orbit radius	R = 5.06 m
Revolution frequency	f_o = 1.259 MHz
Betatron ν values	ν_x = 2.250
	ν_y = 2.250
Vacuum pressure	1×10^{-10} torr
Injection scheme	Multiturn injection
Magnet and Lattice	
Number of normal cells	8
Number of superperiods	8
Number of long straight sections	8
Periodic structure	Q_F B Q_D $\bar{0}$
Bending magnets	
Number	8
Gap	70 mm
Pole width	258 mm
Good field aperture	40 × 170 mm^2
Quadrupole magnets	
Number	16
Length	0.20 m
Field gradient	k_F = 0.240 kG/cm
	k_D = 0.435 kG/cm
Momentum compaction factor	
	Maximum = 1.70 m
	Minimum = 1.01 m
	Average = 1.41 m
Betatron amplitude function	(x) (ν)
Maximum	= 4.94 m 5.51 m
Minimum	= 1.08 m 1.18 m
RF Stacking System	
Frequency	8.81 MHz
Harmonic number	7
Maximum accelerating voltage	1.1 kV
Number of cavities	1
Total RF power	1.3 kW
Stacking parameter	
Momentum spread of the stacked beam	2.469 %
Momentum difference between the injection orbit and stack top	6.289 %
Repetition rate	50 Hz
Maximum RF stacking number	100

deeply enough, and the calibration of the Hall probe was executed simultaneously. The effective edge of the field was calculated by the integration of the curve of the fringing field along the beam orbit as shown in Fig.3. The uniformity of the field along the radial direction was measured at the sufficiently inner side of the magnet gap from the edge and was better than $\pm 2 \times 10^{-4}$ over the whole useful aperture.

The field gradient of the quadrupole magnet was measured with twin coils translated horizontally and the induced voltage at each coil was fed into a VFC circuit of high sensitivity.[6] The deviation of the field gradient along the radial direction was measured and was found to be less than 0.5 % in a whole region from x = - 85 to + 85 mm, where x denotes the distance from the central axis of the magnet as shown in Fig.4. The deviation of the effective length of the focusing action was also measured by the longer twin coils and was found to be less than 1 % over the above region. The effective length was calculated to be 260 mm, while the geometrical one is 200 mm.

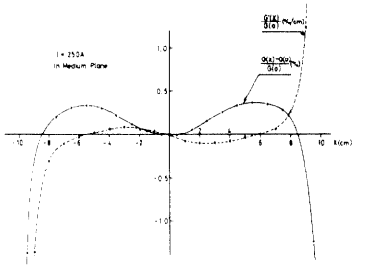

Fig.4. The field gradient of the quadrupole magnet (——), and the sextupole component (---) along the beam orbit. The value of G(0) is 0.44 kG/cm.

3. Multiturn Injection and RF Stacking

A combination of multiturn injection and RF stacking,[7,8,9] is applied to the TARN. In this injection method, heavy ions from the cyclotron are injected via a magnetic and an electrostatic inflectors while are excited two bump magnets, and then, stacked in a longitudinal phase space by an RF field. This injection scheme is very efficient for obtaining higher beam intensity.

Multiturn Injection Method

For this injection scheme, two pulse magnets are located upstream and downstream from the injecting position. These magnets produce a bump in the closed orbit between them and the distance between the magnets should be a half of betatron wave-length in order to avoid any effect on other parts of the equilibrium orbit. The rate and the collapsing rate of the closed orbit distortion is determined so as to optimize the beam intensity stacked in the transverse phase space.

Assuming a constant collapsing rate of the bump field, the inflector septum moves by a constant distance in the transverse phase space at every revolution period. Thus, an acceptance seen by the injector beam at a particular instant, which is defined as a partial acceptance, changes its location, shape and area throughout the injection period.

If the beam emittance is large, the injected particles are possible to populate throughout the partial acceptance, and therefore, the acceptance ellipse is filled with heavy ions except for the region shadowed by the septum.

In the case of larger acceptance, however, the effect of the finite beam emittance becomes serious. The filling factor, which is defined as a ratio of populated area to the acceptance, decreases with increasing acceptance.

A betatron phase advance between the center of the upstream bump magnet and the injecting position also affects on the filling factor.

Taking into account these effects, a calculation was carried out and results are used in the following sections.

RF Staking Method

A procedure of the RF stacking in the TARN is similar to the one which is used for the stacking of high energy proton beams at ISR, CERN.[10] The beam is injected into the TARN by a multiturn method as described above. The area of the longitudinal phase space of the injected beam is estimated considering the energy and phase spreads of the cyclotron beam. Energy spread, $\Delta T/T$, and phase spread, $\Delta\phi$, of the beam from the cyclotron was measured at less than 2×10^{-3} and $\pm 2°$, respectively, where T denotes a kinetic energy of nucleon. Then the phase space area of the beam is 0.88 (rad.keV).

The initial voltage of an RF field is determined to be such a value as the separatrix well cover the phase space area of the injected beam and is rather freely chosen within the limits of satisfying the above condition. Then the RF voltage at the capture process is chosen as the same value at the acceleration period, 1100 V, at which the period of phase oscillation is 1.13 msec.

The rate of change of momentum for the synchronous particle, $\frac{\Delta P/dt}{P}$, is designed at 1.52×10^{-2} (ms^{-1}) for the synchronous phase angle of 30° and RF voltage of 1100 V. The fractional momentum variation corresponding to the distance from the injection orbit is 3.82 %. Then it is required 2.5 ms to change the momentum of the injected beam to that of the bottom of the stacked beam. The revolution-frequency difference between the injected and stacked beam at the bottom is 32.6 kHz and the corresponding RF frequency difference is 228 kHz.

During a period of acceleration from the bottom to the top of the stacked region, the RF voltage is adiabatically reduced to the final voltage. This reduction of RF voltage is necessary because the high RF voltage brings about undesirable large momentum spread of the stacked beam when the separatrix is moved to the top of the stacking orbit.

The final voltage is determined so that the area of the separatrix is just equal to or larger than the longitudinal phase space area of the injected beam, 0.88 (rad·keV). However this reduction requires a much longer time, for example 2 s, for the deposit period. This is because, first, the adiabaticity in the change of RF voltage is required and, second, the synchronous phase angle must be kept constant at 30° during a process of deposit. On the other hand beam life time in the ring is determined by the pressure in the vacuum chamber, say 1×10^{-10} torr, and is estimated at 1 sec for the survival rate of 90 % for this pressure. Then slow repetition rate of RF stacking may result in a low intensity in the ring. Typical stacking rate is 50 Hz and the final voltage is 100 V for this repetition rate. The RF voltage is reduced adiabatically and the necessary time to change from the initial bucket to the final one is designed as 6.3 ms.

Momentum difference between the bottom and the top of the stacked beam is designed as 2.469 % and hence the RF frequency must be changed by 149 kHz for this acceleration. In order to keep $\sin\phi_s = 0.5$ for the RF voltage of 100 V during the acceleration, the time derivative of the frequency must be 8.8 kHz/ms and then the time required for the deposit is 17 ms.

At every acceleration, the bucket passes over the stacked particles and disturbs their energy oscillations. The mean beam energy decrease ΔE of the stacked beam can be derived from Liouville's theorem:

it is found that after n passages

$$\Delta E = 3.75\ n\ (keV)\ .$$

The permissible energy spread for the beam stacking is designed as 392 (keV) and therefore the maximum possible stacked number is calculated at 104.

The energy dispersion $\langle\delta E\rangle$ introduced in an initially monoenergetic beam due to the n passages of the bucket is given by

$$\langle\delta E\rangle = \sqrt{n}\ \delta E_{st} \cdot \sin\phi_s\ ,$$

where δE_{st} represents an energy width of a stationary bucket. The numerical result is $\langle\delta E\rangle$ = 56.4 keV and the ratio of $\langle\delta E\rangle$ to ΔE is 0.14 which appears to be quite acceptable.

Combination of Multiturn Injection and RF Stacking Method

Using the results of the above calculations, a total stacking number both in transverse and longitudinal phase spaces are obtained as a function of a half aperture offered for the multiturn injection. The total stacking number has the maximum value of about 1900 at x_0 = 20 mm. The calculated envelopes of multiturn injected and RF stacked beams are shown in Fig.5 as a function of length along the central orbit.

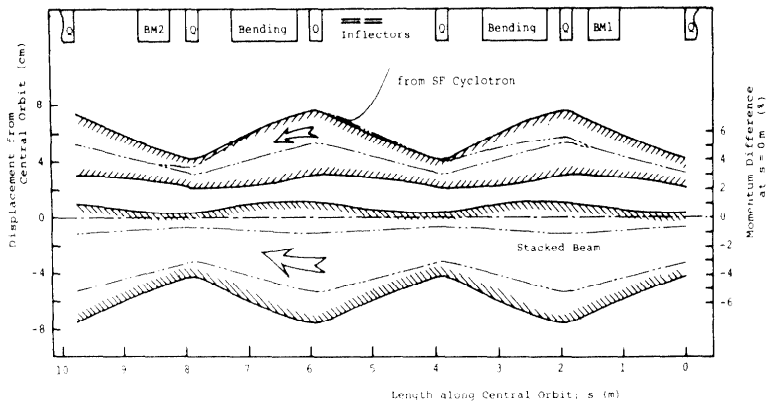

Fig.5. The envelopes of multiturn injected and RF stacked beams (——). The closed orbits of heavy ions with momenta different from that of central oribt beam are also shown (—··—).

4. RF System, Beam Monitor and Control

The RF system is composed of a low level RF electronics system and high power parts including an accelerating cavity. The low level RF electronics plays an important role to obtain phase lock mechanism between beam and RF accelerating field. Also it is used to control the accelerating voltage and frequency so as to obtain the optimum RF stacking condition. Programmed accelerating voltage and frequency are illustrated in Fig.6.

The amplitude of the RF field is modulated by a balanced modulator in accordance with the waveform from a function generator. The fast feedback voltage control function is given by an amplitude normalizer. It stabilizes the RF voltage against the variation of the cavity impedance due to the sweep of the frequency.

The phase difference between the accelerating field and the fundamental mode of the bunch signal is measured by a phase detector, where the beam phase information is derived from a core-type beam monitor with a resonator whose resonant frequency is adjusted at the RF frequency. The output signal of the phase detector is fed to a voltage controlled oscillator (VCO) through a summing amplifier. The output frequency of the VCO is determined by the voltage on a varacter, which is composed of a program term from the function generator and feedback one coming from the phase detector. The absolute value of the stable phase angle is determined by a phase shifter in the loop.

An accelerating structure is composed of two cavities with an electrical length of a quarter wave. In order to tune the cavity over an operating frequency and to reduce the size of the cavity, 24 ferrite rings, 382 mm O.D., 260 mm I.D. and 20 mm thick, are stacked in the cavity. Each ferrite ring is sandwitched by cooling copper discs. Electrical characteristics of several ferrite materials were investigated, and the ferrite with the highest μQf value was selected. The resonant frequency of the cavity is varied by changing a capacitance between two inner conductors or by impressing the biasing magnetic field in the ferrite cores. The two-turn bus bars were folded around the ferrite rings.

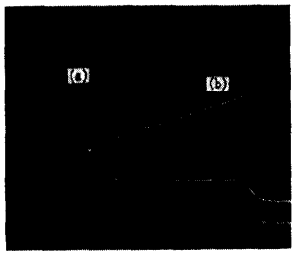

Fig.6. (a) Programmed accelerating voltage at the low level electronics. It rises from 0 V to 4.5 V and stays at 0.5 V. (b) Accelerating frequency, which varies from 8.5 MHz in a range of 380 kHz. The time scale is 2 ms/div.

The RF power is fed to the cavity by a 5 kW RF power amplifier through a wide band transformer of a transmission type for the matching of their impedances. The transformer was also used to obtain two RF fields, whose phases are different by 180° from each other for the push-pull operation of the cavity.

Several kinds of beam monitors were prepared for efficient beam handling during an injection and stacking. Electrostatic monitors and magnetic ones using ferrite cores were used as non-destructive type, which is necessary for beam stacking. The former detects beam position measuring asymmetry of induced charges on two electrodes. Signals are fed through ADC circuits into a mini-computer, FACOM PFU-400, where the position is calculated from the two pulse heights and the result is recorded. The information is served for the control of RF acceleration. The magnetic monitor, where a coil picks up magnetic flux induced in the ferrite core, provides informations on beam intensity and phase. Output signals are converted into sine-wave through a tank circuit and fed to the RF control system. Four beam-dumping (Faraday-cup type) monitors are installed in the ring for the study of the injection orbit of the beam in the ring. This detector, with sixteen strips of Be-Cu foil 500 μm in thickness and 2 mm in width, measures intensity and position simultaneously.

The control system regulates the RF system, logs data from various systems (beam transport, vacuum, magnet and beam monitoring systems), and gives an alarm for abnormality in above systems. The system is provided with two mini-computers where the former is for the RF system and the latter for data logging and alarming. The acquired data are to be analyzed to learn the characteristics of the TARN and to search the best condition for the operation.

5. Vacuum System

On-beam pressure lower than 1×10^{-10} torr (1.33×10^{-8} Pa) is required to achieve 90 % survival probability of accumulated ions during a period of 1 sec.[11] Since 1976, some preliminary tests on ultra-high vacuum (UHV) system have been carried out, where two test stands for UHV studies were constructed. The vacuum chamber of test stand I is cylindrical, 30 cm in diameter and 200 cm in length, and is made of stainless steel 316L. The pumping system is composed of a 1500 ℓ/s titanium sublimation pump with liquid nitrogen shroud, and a 500 ℓ/s turbomolecular pump backed by a 400 ℓ/s oil diffusion pump. On the other hand, the vacuum chamber of test stand II is a prototype scaled model of the bending section and the short straight section in the TARN. The pumping system is composed of a 400 ℓ/s sputter-ion pump and a 200 ℓ/s turbomolecular pump backed by a 100 ℓ/s turbomolecular pump. The backing and the discharge cleaning effects were measured using the test stand I and II, respectively.

Pumping characteristics have been studied to establish efficient procedures for baking out the vacuum chamber and glow discharge cleaning in Ar or Ar + O_2. It is found that the partial pressure of H_2O decreases significantly after glow discharge processing. In the typical spectrum, a peak at m/e = 16 was the highest one. It may be understood that this peak is not due to ions in gas-phase, but to O^+ ions emitted from the surface of the quadrupole mass-filter caused by electron impact desorption effect.[12] This peak is a very useful indicator of "cleanliness" of the surface in the system.

In November 1978, the whole vacuum system was assembled tentatively prior to installation into the magnet gaps. The system was baked at 250°C for 50 hours, and the average pressure of 2×10^{-11} torr was attained after 1,000 hour pumping down without glow discharge processing.

The drawing of the system is shown in Fig.7. The

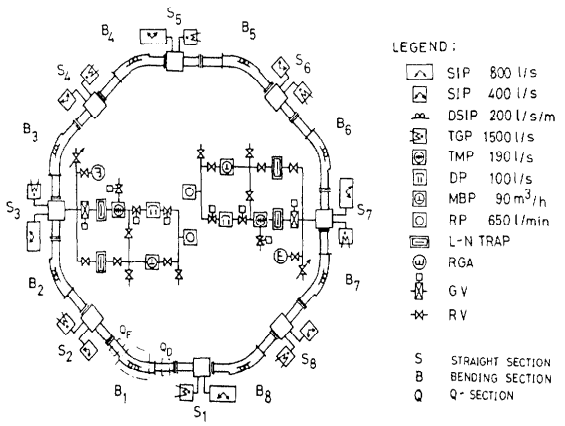

Fig.7. Vacuum system of the TARN

chamber has a circumferencial length of 31.8 m, and is divided into eight unit sections, each of which consists of one dipole magnet chamber of 45×234 mm^2 rectangular cross section, two quadrupole magnet chambers of 90×190 mm^2 diamond-shaped cross section, and a straight section chamber. These chambers are made of stainless steel 316L. Each pumping system is composed of a sputter-ion pump, a titanium sublimation pump, and a distributed pump, which is installed along the inside of outer wall of the dipole magnet chamber and is also used as a high-voltage electrode for in situ glow discharge cleaning.[13]

As shown in Fig.7, two roughing and auxiliary pumping systems are located at the straight sections S-3 and S-7, each of which comprises a turbomolecular pump backed by either an oil diffusion pump or a mechanical booster pump, and a rotary pump.

The straight section S-1 is connected to the injection beam transport line through three stages of differential pumping system.

6. Beam Transport and Injection System

Heavy ions from the injector cyclotron are introduced to the TARN via a transporting path with optical matching elements and beam monitoring devices. The layout of the beam transport is illustrated in Fig.1. The beam transporting system is divided into four sections; 1) momentum analyzing section with two bending magnets of 90° and 78.30° deflection angles, respectively, and three pairs of quadrupole magnets, 2) momentum matching section with a bending magnet of 71.17° deflection angle and one quadrupole pair where each element has a function to produce a double achromatic beam, that is to say, both the momentum dispersion function and its gradient are vanished, 3) dispersion-free matching section of the transverse phase ellipses with two quadrupole pairs, 4) momentum matching section which produces a required dispersion at the injection point of the ring. Analysis of the beam optics was performed with the aid of the computer program MAGIC.

Analyzing magnets, named BA1 and BA4, are of the modified window-frame type with edge focusing function. The shapes of pole edges at entrance and exit are approximated to Rogowski's curve and field clamps are attached to the edges.

Time structure of the incident beam to the TARN is controlled by the kicker magnet of the deflection angle of 0.0745°, by which beam width is set to 20 ∿ 100 μs.

Injection Apparatus

The electrostatic inflector system consists of two sets of electrodes and three probes. The electrodes of negative potential are made of stainless steel and supported by ceramic insulators whereas the septum electrodes are tantalum foils of 0.1 mm thick. The gap of electrodes is designed to be 8 mm, and the maximum electric field strength in the gap is 100 kV/cm. The length of each electrode along the beam path is 30 cm. These four electrodes are mounted on one movable base plate made of stainless steel.

The bump magnets are made of ferrite, and has a cross section of C-type. The pole has a length of 40 cm and a width of about 20 cm. Shims are disposed on the poles in order to obtain the most desirable drop-off of field strength. The pole gap is 50 mm and the required field strength at the pulse peak is 274 G. The magnetic field is generated by a two-turn coil which has an inductance of about 9 μH.

The high-current pulse-forming circuit consists of charging condensors, magnet coil itself, and resistors with diode in series. A high-voltage and high-current SCR is used as a switching element. By the condensor and the resistors, the bump decay time is varied from 20 to 50 μs.

Acknowledgments

The authors express their sincere gratitude to Professors K. Sugimoto and M. Sakai for their encouragement and support during the work. They are indebted to Dr. K. Sato, Professor M. Sekiguchi and members of the cyclotron group for their collaboration in the construction of the beam transport line. They are grateful to Professor K. Kaneko and Mr. T. Morimoto for their collaboration at the early stage of the vacuum study. Thanks are also due to Mr. T. Fujino and members of the machine shop for their assistances in designing and constructing many parts of the ring.

They used the computers TOSBAC-3400 at INS, HITAC -8800 at KEK and FACOM 230/75 at IPCR in computational calculations.

References

1) Y. Hirao et al., "NUMATRON" INS-NUMA-5, 1977.
2) Y. Hirao, "Numatron Project", Proc. of the Int. Conf. on Nuclear Structure, p.594 (1977).
3) Y. Hirao et al., "The INS 176 cm Sector Focusing Cyclotron", Proc. 7th Int. Conf. on Cyclotrons and Their Applications, p.103 (1975).
4) K. Sato et al., "Status of the 176 cm Sector Focusing Cyclotron", Proc. 8th Int. Conf. on Cyclotrons and Applications (1978).
5) M. Kumada et al., "Wide Aperture Q Magnet with End Cut Shaping", Proc. of 2nd Symp. on Acc. Sci. and Tech., p.75 (1978).
6) M. Kumada et al., "Flux Meter for Field Gradient with Pendulum", Proc. of 2nd Symp. on Acc. Sci. and Tech., p.73 (1978).
7) E. Keil, "Stacking in Betatron Phase Space for the ISR", ISR-TH/67-10.
8) T. Katayama and S. Yamada, "Injection Method of the NUMATRON", Proc. of the 2nd Symp. on Acc. Sci. and Tech., p.151 (1978).
9) S. Yamada and T. Katayama, "Injection and Accumulation Method in the TARN", INS-NUMA-12 (1979).
10) For example W. Schnell, Proc. of Conf. on High Energy Acc., Dubna (1963).
11) K. Chida et al., "Vacuum System of the Test Ring for the NUMATRON", Proc. of the 2nd Symp. on Acc. Sci. and Tech., p.35 (1978).
12) P. A. Redhead, "Ion Desorption by Electron Bombardment; Relation to Total and Partial Pressure Measurement", J. Vac. Sci. Technol. Vol.7, No.1, 182 (1970).
13) A. G. Mathewson, J. Kouptsidis and L. Hipp, Proc. 7th Int. Vac. Congr. and 3rd Int. Conf. Solid Surfaces, Vienna, 1977.